IL NUOVO CIMENTO Vol. 114 B, N. 11 Novembre 1999

Coaxial-wire technique: A comparison between theory and experiment

D. Davino([1])([2]), M. R. Masullo([1]), V. G. Vaccaro([1])([3]) and L. Verolino([1])([2])

([1]) *INFN, Sezione di Napoli - I-80126 Napoli, Italy*
([2]) *Dipartimento di Ingegneria Elettrica - Via Claudio 21, I-80125 Napoli, Italy*
([3]) *Dipartimento di Scienze Fisiche - I-80126 Napoli, Italy*

(ricevuto l'8 Aprile 1999; approvato il 23 Settembre 1999)

Summary. — The measurement of the scattering matrix inside the coaxial-wire technique is an entry parameter for the calculation of the longitudinal coupling impedance of an accelerating machine. In order to optimise the method of measuring scattering matrices we propose, first, a mathematical technique which allows us to know in advance the most precise coefficients of this matrix for a simple and realistic case. Keeping this as a reference point, we then describe a measuring procedure which gave results in a very good agreement with the theory.

PACS 41.20.Jb – Electromagnetic wave propagation; radiowave propagation.
PACS 84.40.Az – Waveguides, transmission lines, striplines.
PACS 06.90 – Other topics in metrology, measurements, and laboratory procedures.

1. – Introduction

Both longitudinal and transverse impedances [1-3] are key parameters for the design of accelerators. Actually, in order not to trigger offensive instabilities, the machine impedances must be kept, within a certain margin, inside the impedance budget. This budget is found by means of stability criteria [4], while the margin is chosen according to the reliability of the prediction for the amount of impedance of all machine devices. Among the prediction methods, the one based on bench measurements by means of stretched wire is the most attractive because of its simplicity. This method resorts to the measurement of the scattering ($\boldsymbol{S}$) matrix which, by means of *ad hoc* manipulations [5], gives the value of the device under test (DUT) impedance. We neglect for the moment the discussion and analysis of the procedure which lead from $\boldsymbol{S}$-matrix to the DUT impedance. This argument has been widely treated in the literature [6-8] and it will be the argument of a forthcoming paper.

In this work we want to compare the scattering matrix, theoretically derived, of a simple and realistic device with ohmic losses, with the one measured with coaxial-wire method. This to the end of improving the measurement techniques mainly in the range

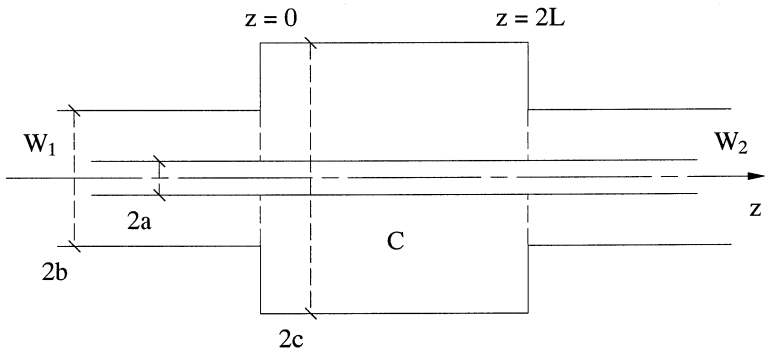

Fig. 1. – Geometry of the cavity powered by a circular coaxial waveguide.

of frequencies where the DUT length is comparable or larger than the wavelength. It has to be underlined that, for a reliable comparison, we need also a very precise theoretical tool. The choice of a simple test structure for the measure is due to this end both for experimental reasons and for theoretical approach.

We will, therefore, present and use a new technique for finding the generalised scattering matrix of a DUT where a thin wire is stretched on the axis for simulating the bunch passing through. As is well known, the concept of the generalised scattering matrix is very closely related to the scattering matrix of circuit theory or of the microwave network theory [9]. However, it differs from the conventional scattering matrix since it is extended to consider evanescent as well as propagating modes in the waveguides so that each element of the $\boldsymbol{S}$-matrix is an infinite matrix itself. This approach enables us to attack a class of boundary-value problems of guided waves and in particular it is suitable for studying structures in which are present two or more geometrical discontinuities (like step, iris). Their geometry is such that a generalised scattering matrix description for each of these structures can be conveniently derived. This enables one to express the solution of the problem in terms of a Neumann series involving matrices of infinite order, the solution being formally exact [10].

A complete analysis of the coupling between a rectangular waveguide and an open cavity has been developed [11], considering the relevant eigenfunctions in the waveguide and in the cavity. The mode matching technique (MMT) proposed here represents an extension of that analysis because the coupling between the feeding waveguide and the cavity is treated in such a way to take into account all the longitudinal modes of the cavity. The factorized form of the field in a cavity can be used in order to evaluate the series related to the longitudinal modes and to obtain an accurate solution by truncating the infinite matrices to a reasonably small size. Furthermore with the MMT we are able to introduce ohmic losses in the test structure in a non-perturbative way.

In order to test the technique, we examine a cylindrical pill-box cavity powered by two coaxial waveguides as shown in fig. 1. We suppose that, except the fundamental mode, a TM electromagnetic field propagates along the waveguides and, as a consequence, in the cavity. In this way we are able to investigate, without loss of generality, a structure useful in accelerator physics, on which a coaxial wire bench measurement can be performed. The scattering matrix is measured by introducing on the DUT axis a small conductive wire on which a current pulse of the same shape of the bunch is riding [5].

As a matter of fact these applications need a reliable and effective description of both

the resonant modes and the coupling between the cavity and the feeding system.

2. – Representation of the field in the cavity

The electromagnetic field inside a cavity can be expressed in terms of a complete set of basis functions [12]

$$\vec{E}\,(P) = \sum_i V_i\,\vec{E}_i\,(P), \quad \vec{H}\,(P) = \sum_i A_i\,\vec{H}_i\,(P)\,, \tag{2.1}$$

where the coefficients V_i and A_i are independent of the coordinates. If the dielectric filling the cavity is homogeneous and isotropic and the expansion functions, $E_i(P)$ and $H_i(P)$, are orthogonal, it can be shown [12] that the expansion coefficients are given by

$$A_i = \frac{1}{k^2 - k_i^2}\left[\frac{jk}{\zeta_0}\oint_S \hat{n}\times\vec{E}\cdot\vec{H}_i^{\,*}\,\mathrm{d}S + k_i\oint_S \hat{n}\times\vec{H}\cdot\vec{E}_i^{\,*}\,\mathrm{d}S\right], \tag{2.2}$$

$$V_i = \frac{1}{k^2 - k_i^2}\left[k_i\oint_S \hat{n}\times\vec{E}\cdot\vec{H}_i^{\,*}\,\mathrm{d}S - jk\zeta_0\oint_S \hat{n}\times\vec{H}\cdot\vec{E}_i\,\mathrm{d}S\right],$$

where S is the cavity surface, whose normal unit vector $\hat{n}$ is, as usual, oriented outside the integration domain, $*$ denotes the complex conjugate, k_i are the cut-off propagation constants and ζ_0 is the characteristic impedance of medium filling the waveguide.

Due to the symmetry of the structure we examine only TM modes. The rotational symmetry implies the use of two indexes in the expansions (2.1)

$$\vec{E}\,(r,z) = \sum_{p,s} V_{ps}\,\vec{E}_{ps}\,(r,z), \quad \vec{H}\,(r,z) = \sum_{p,s} A_{ps}\,\vec{H}_{ps}\,(r,z)\,, \tag{2.3}$$

where the subscript p characterises the transverse modes, whereas s defines the longitudinal ones. For a closed cylindrical cavity of length $2L$, it is well known that [12] the expansion functions assume the factorized form

$$\vec{H}_{ps}\,(r,z) = \sqrt{\frac{\varepsilon_s}{2L}}\,\Phi_p^{\mathrm{c}}(r)\cos(k_s z)\hat{\varphi}\,, \tag{2.4}$$

where Neumann's symbol $\varepsilon_s = 1$, if $s = 0$, $\varepsilon_s = 2$, if $s = 1, 2, 3, \ldots$ and

$$k_s = \frac{\pi s}{2L} \quad (s = 0, 1, 2, \ldots)$$

have been introduced. The transverse modal functions $\Phi_p^{\mathrm{c}}(r)$ are related to transverse eigenvalues (the apex c stays for cavity) and have the functional form([1]) for a coaxial

([1]) The subscript 1 indicates the fundamental mode, whereas $p = 2, 3, \ldots$ indicates the higher-order modes.

guide with c and a, respectively, outer and inner radii:

$$\Phi_p^{\mathrm{c}}(r) = \begin{cases} \dfrac{1}{r\sqrt{2\pi \ln(c/a)}} & p = 1\,, \\ \dfrac{x_p\sqrt{\pi}}{2a} \dfrac{J_1(rx_p/a)Y_0(x_p) - J_0(x_p)Y_1(rx_p/a)}{\sqrt{J_0^2(x_p)/J_0^2(cx_p/a) - 1}} & p = 2, 3, \ldots, \end{cases} \tag{2.5}$$

the cut-off propagation constants are given as

$$k_{ps}^2 = k_s^2 + (x_p/a)^2\,, \tag{2.6}$$

and x_p is the p-th solution of the equation

$$x[J_0(\alpha x)Y_0(x) - J_0(x)Y_0(\alpha x)] = 0\,, \tag{2.7}$$

with $\alpha = c/a$. Moreover the expansion coefficients assume the simplified form [12]

$$\zeta_0 A_{ps} = \frac{jk}{k^2 - k_{ps}^2} \oint_S \hat{n} \times \vec{E} \cdot \vec{H}_{ps}^{*}\, \mathrm{d}S, \quad V_{ps} = -\frac{jk_{ps}}{k}\zeta_0 A_{ps}\,. \tag{2.8}$$

Note explicitly that the tangential electric field appearing in eq. (2.8) is the actual field over S. It is not given by the first of expressions (2.3), which, differently from the expression for the tangential magnetic field, does not provide a representation for the tangential component uniformly valid up to cavity boundaries.

3. – Representation of the field in the waveguides

It is well known that the study of the electromagnetic field inside a propagating structure can be performed by a separation of the electromagnetic field according to the longitudinal (along z) and transverse components (the subscript t stays for transverse) [12, 13]

$$\vec{E}\,(P) = \vec{E}_{\mathrm{t}}\,(P) + E_z(P)\hat{z}, \quad \vec{H}\,(P) = \vec{H}_{\mathrm{t}}\,(P) + H_z(P)\hat{z}\,. \tag{3.1}$$

Introducing a polar system of coordinates (r, φ) in the transverse section and referring to TM modes ($H_z = 0$), we can write the electromagnetic field by means of the following modal expansion:

$$\vec{E}_{\mathrm{t}}\,(r,\varphi) = \sum_n V_n(z)\,\vec{e}_{\,n}\,(r,\varphi), \qquad E_z(r,\varphi) = \frac{\zeta_0}{jk}\sum_n k_n A_n(z)\Phi_n(r,\varphi)\,, \tag{3.2}$$

$$\vec{H}_{\mathrm{t}}\,(r,\varphi) = \sum_n A_n(z)\,\vec{h}_{\,n}\,(r,\varphi), \qquad H_z(r,\varphi) = 0\,,$$

where $\vec{e}_{\,n}\,(r,\varphi)$ and $\vec{h}_{\,n}\,(r,\varphi)$ are the vector mode functions, whereas $V_n(z)$ and $A_n(z)$ are the scalar ones, k_n is the transverse eigenvalue, k is the propagation constant [12, 13].

The scalar mode functions have to obey the "telegraphers" equations and therefore the transverse fields can be rewritten [12, 13] as

$$(3.3)\quad \vec{E}_{\mathrm{t}}\,(r,\varphi)=\sum_n [V_n^+(z)+V_n^-(z)]\;\vec{e}_{\,n}\,(r,\varphi),\;\vec{H}_{\mathrm{t}}\,(r,\varphi)=\sum_n \frac{V_n^+(z)-V_n^-(z)}{\zeta_0\zeta_n^{\mathrm{w}}}\;\vec{h}_{\,n}\,(r,\varphi),$$

namely as a superposition of forward waves $V_n^+(z)$ and of backward ones $V_n^-(z)$; the modal impedance ζ_n^{w} is given by

$$(3.4)\qquad \zeta_n^{\mathrm{w}}=\frac{\sqrt{(ka)^2-w_n^2}}{ka}\,,\quad w_n\le ka,\quad \zeta_n^{\mathrm{w}}=-j\frac{\sqrt{w_n^2-(ka)^2}}{ka}\,,\quad w_n\ge ka\,,$$

where the apex w stays for waveguide and w_n are real zeros of the equation

$$(3.5)\qquad x[J_0(\alpha x)Y_0(x)-J_0(x)Y_0(\alpha x)]=0,\quad \text{with}\quad \alpha=b/a\,,$$

with a the inner waveguide radius and b the outer one.

In order to simplify the mathematical treatment of the problem, we examine an axial symmetric case, so the functional dependence on φ will be omitted in the following. As a consequence, using the property of the vector mode orthogonality for $\vec{e}_{\,n}$ and $\vec{h}_{\,m}$ one can evaluate these functions for a coaxial cable [13],

$$(3.6)\qquad \vec{e}_{\,m}\,(r)=\hat{r}\Phi_m^{\mathrm{w}}(r),\quad \vec{h}_{\,m}\,(r)=\hat{\varphi}\Phi_m^{\mathrm{w}}(r)\,,$$

where $\Phi_m^{\mathrm{w}}(r)$ is the linear combination of Bessel functions

$$(3.7)\quad \Phi_m^{\mathrm{w}}(r)=\begin{cases}\dfrac{1}{r\sqrt{2\pi\ln(b/a)}}\,, & m=1\,,\\[2ex] \dfrac{w_m\sqrt{\pi}}{2a}\dfrac{J_1(rw_m/a)Y_0(w_m)-J_0(w_m)Y_1(rw_m/a)}{\sqrt{J_0^2(w_m)/J_0^2(bw_m/a)-1}} & m=2,3,\ldots.\end{cases}$$

Let us finally note that the expression (3.7) for the waveguide is similar to the one (2.5) for the cavity.

4. – Waveguide-cavity coupling

In the above field expressions (2.8) and (3.3), coefficients A_{ps} and $V_n^{\pm}$ are unknown quantities, which can be obtained by imposing the field matching, namely the continuity of the tangential component of the magnetic and electric field on the coupling apertures, S_1 ($z=0$ and $a\le r\le b$) and S_2 ($z=2L$ and $a\le r\le b$). This cannot be explicitly done for the tangential component of the electric field because of the non-uniform convergence of the first expansion (2.3) on the cavity boundaries: the tangential component of the electric field in the cavity vanishes on the boundaries. Instead the continuity of the tangential component of the magnetic field over the coupling aperture S_1 ($z=0$ and $a\le r\le b$) gives

$$(4.1)\qquad \sum_{p,s}\sqrt{\frac{\varepsilon_s}{2L}}A_{ps}\Phi_p^{\mathrm{c}}(r)=\frac{1}{\zeta_0}\sum_q\frac{V_{1q}^+-V_{1q}^-}{\zeta_q^{\mathrm{w}}}\Phi_q^{\mathrm{w}}(r),\quad r\in S_1\,,$$

where expansion (3.3) of the tangential component of the magnetic field in the waveguide, and representation (2.3) of the magnetic field in the cavity have been used. We called for brevity $V_q^+(0) = V_{1q}^+$ and $V_q^-(0) = V_{1q}^-$. Similarly the matching over the aperture S_2 ($z = 2L$ and $a \leq r \leq b$) gives

$$\sum_{p,s}(-1)^s \sqrt{\frac{\varepsilon_s}{2L}} A_{ps} \Phi_p^{\mathrm{c}}(r) = -\frac{1}{\zeta_0} \sum \frac{V_{2q}^+ - V_{2q}^-}{\zeta_q^{\mathrm{w}}} \Phi_q^{\mathrm{w}}(r), \quad r \in S_2\,, \tag{4.2}$$

where $V_q^+(2L) = V_{2q}^+$ and $V_q^-(2L) = V_{2q}^-$. Both relations (4.1) and (4.2) are valid for $a \leq r \leq b$; so we can project them on the complete set of the coaxial cable modes $\Phi_q^{\mathrm{w}}(r)$, obtaining the following system of equations:

$$V_{1q}^+ - V_{1q}^- = \zeta_0 \zeta_q^{\mathrm{w}} \sum_{p=1}^{\infty} C_{pq} \sum_{s=0}^{\infty} \sqrt{\frac{\varepsilon_s}{2L}} A_{ps} = \zeta_0 \zeta_q^{\mathrm{w}} \sum_{p=1}^{\infty} C_{pq} (A_p^E + A_p^O)\,, \tag{4.3}$$

$$V_{2q}^- - V_{2q}^+ = \zeta_0 \zeta_q^{\mathrm{w}} \sum_{p=1}^{\infty} C_{pq} \sum_{s=0}^{\infty} (-1)^s \sqrt{\frac{\varepsilon_s}{2L}} A_{ps} = \zeta_0 \zeta_q^{\mathrm{w}} \sum_{p=1}^{\infty} C_{pq} (A_p^E - A_p^O)\,, \tag{4.4}$$

where the coefficients C_{pq}, defined and evaluated in the appendix A, take into account the coupling among the waveguide and the cavity modes. Furthermore the two series A_p^E and A_p^O implicitly defined in eqs. (4.3) and (4.4) could be expressed in a closed form.

In order to investigate the electromagnetic coupling between the waveguides and the cavity, we have to evaluate the expansion coefficients A_{ps} given by the integrals (2.8) and therefore to know the electric field on the cavity surfaces. If we assume that both the cavity and the waveguides are perfectly conducting, the contribution to the coefficient value (2.8) comes only from the coupling apertures, that is

$$\zeta_0 A_{ps} = \frac{jk}{k^2 - k_{ps}^2} \int_{S_1 + S_2} \hat{n} \times \vec{E} \cdot \vec{H}_{ps}^{\,*}\, \mathrm{d}S\,. \tag{4.5}$$

As already noted above, the tangential component of the electric field cannot be obtained on the cavity boundary by means of the representation (2.3). This difficulty can be overcome by the modal expansion (3.3) and because of the continuity of the tangential component of the electric field it is

$$\zeta_0 A_{ps} = \frac{jk}{k^2 - k_{ps}^2} \sqrt{\frac{\varepsilon_s}{2L}} \sum_{t=1}^{\infty} [(-1)^s (V_{2t}^+ + V_{2t}^-) - V_{1t}^+ - V_{1t}^-] C_{pt}\,, \tag{4.6}$$

where, as before, the coefficients C_{pt} are in Appendix A. The relation (4.6) delineates an explicit dependence on the index s of the coefficients A_{ps}. This fact implies that we are able to get for the two series appearing in (4.3) and (4.4) the following expressions [14]:

$$A_p^E = j \frac{\operatorname{ctg}(kL\zeta_p^{\mathrm{c}})}{2\zeta_0 \zeta_p^{\mathrm{c}}} \sum_{t=1}^{\infty} [V_{2t}^+ + V_{2t}^- - V_{1t}^+ - V_{1t}^-] C_{pt}\,, \tag{4.7}$$

$$A_p^O = j \frac{\operatorname{tg}(kL\zeta_p^{\mathrm{c}})}{2\zeta_0 \zeta_p^{\mathrm{c}}} \sum_{t=1}^{\infty} [V_{2t}^+ + V_{2t}^- + V_{1t}^+ + V_{1t}^-] C_{pt}\,. \tag{4.8}$$

In this way, from a physical point of view, we have taken into account all the longitudinal modes of the cavity. Substituting sums (4.7) and (4.8) into relations (4.3) and (4.4) respectively, we get a system containing only the powering waves:

$$(4.9)\quad \begin{cases} \boldsymbol{V}_2^- - \boldsymbol{V}_2^+ = \dfrac{1}{2}\boldsymbol{E}(\boldsymbol{V}_2^+ + \boldsymbol{V}_2^- - \boldsymbol{V}_1^+ - \boldsymbol{V}_1^-) - \dfrac{1}{2}\boldsymbol{O}(\boldsymbol{V}_2^+ + \boldsymbol{V}_2^- + \boldsymbol{V}_1^+ + \boldsymbol{V}_1^-)\,, \\ \boldsymbol{V}_1^+ - V_1^- = \dfrac{1}{2}\boldsymbol{E}(\boldsymbol{V}_2^+ + \boldsymbol{V}_2^- - \boldsymbol{V}_1^+ - \boldsymbol{V}_1^-) + \dfrac{1}{2}\boldsymbol{O}(\boldsymbol{V}_2^+ + \boldsymbol{V}_2^- + \boldsymbol{V}_1^+ + \boldsymbol{V}_1^-)\,, \end{cases}$$

where for the sake of simplicity we called

$$(4.10)\qquad \boldsymbol{E} = j\boldsymbol{Z}_{\mathrm{w}}\boldsymbol{C}^T\boldsymbol{Z}_{\mathrm{c}}^{-1}\operatorname{ctg}(kL\boldsymbol{Z}_{\mathrm{c}})\boldsymbol{C}, \quad \boldsymbol{O} = j\boldsymbol{Z}_{\mathrm{w}}\boldsymbol{C}^T\boldsymbol{Z}_{\mathrm{c}}^{-1}\operatorname{tg}(kL\boldsymbol{Z}_{\mathrm{c}})\boldsymbol{C}\,,$$

and we defined the following matrices and vectors:

$$\boldsymbol{C} = [C_{pq}], \quad \boldsymbol{Z}_{\mathrm{w}} = \operatorname{diag}[\zeta_p^{\mathrm{w}}], \quad \boldsymbol{Z}_{\mathrm{c}} = \operatorname{diag}[\zeta_p^{\mathrm{c}}], \quad \boldsymbol{V}_m^{\pm} = [V_{mp}^{\pm},\ m = 1, 2]\,.$$

Before going on, we have to point out some features of our formulation. In the system (4.9) the resonant behaviour of the cavity appears straightforward, and it is included in the two terms $\boldsymbol{O}$ and $\boldsymbol{E}$: the matrix $\boldsymbol{Z}_{\mathrm{c}}^{-1}$ goes to infinity in the case of transverse resonances, meanwhile the cotangent (tangent) terms go to infinity for the longitudinal ones. Our use of field expansions in normal modes has brought us to the useful series (4.7) and (4.8) containing the resonant cavity modes and leading to closed forms. Furthermore, the term $\boldsymbol{Z}_{\mathrm{w}}^{-1}$ contains all the information on the waveguides behaviour.

5. – Scattering matrix

We are now ready to evaluate the generalised scattering matrix. Taking into account that our device under test is symmetric ($S_{11} = S_{22}$) and reciprocal ($S_{12} = S_{21}$), we have to compute only $\boldsymbol{S}_{11}$ and $\boldsymbol{S}_{12}$. We start by getting the difference $\boldsymbol{V}_1^- - \boldsymbol{V}_2^-$, and the sum $\boldsymbol{V}_1^- + \boldsymbol{V}_2^-$ from the system (4.9), that is

$$(5.1)\qquad \begin{cases} \boldsymbol{V}_1^- - \boldsymbol{V}_2^- = (\boldsymbol{I} - \boldsymbol{E})^{-1}(\boldsymbol{I} + \boldsymbol{E})(\boldsymbol{V}_1^+ - \boldsymbol{V}_2^+)\,, \\ \boldsymbol{V}_1^- + \boldsymbol{V}_2^- = (\boldsymbol{I} + \boldsymbol{O})^{-1}(\boldsymbol{I} - \boldsymbol{O})(\boldsymbol{V}_1^+ + \boldsymbol{V}_2^+)\,. \end{cases}$$

As a consequence, it is simple to obtain the generalised scattering matrix

$$(5.2)\qquad \begin{cases} \boldsymbol{V}_1^- = \boldsymbol{S}_{11}\boldsymbol{V}_1^+ + \boldsymbol{S}_{12}\boldsymbol{V}_2^+\,, \\ \boldsymbol{V}_2^- = \boldsymbol{S}_{21}\boldsymbol{V}_1^+ + \boldsymbol{S}_{22}\boldsymbol{V}_2^+\,, \end{cases}$$

where the reflection matrix is defined by

$$(5.3)\qquad \boldsymbol{S}_{11} = \boldsymbol{S}_{22} = \frac{1}{2}[(\boldsymbol{I} + \boldsymbol{O})^{-1}(\boldsymbol{I} - \boldsymbol{O}) + (\boldsymbol{I} - \boldsymbol{E})^{-1}(\boldsymbol{I} + \boldsymbol{E})]\,,$$

and the transmission matrix is given by

$$(5.4)\qquad \boldsymbol{S}_{12} = \boldsymbol{S}_{21} = \frac{1}{2}[(\boldsymbol{I} + \boldsymbol{O})^{-1}(\boldsymbol{I} - \boldsymbol{O}) - (\boldsymbol{I} - \boldsymbol{E})^{-1}(\boldsymbol{I} + \boldsymbol{E})]\,.$$

It is obvious that the reflection (5.3) and the transmission (5.4) matrices are of infinite dimension. In practice, the order of these matrices depends upon the modes propagating through the structure. Performing a numerical elaboration, one has to truncate these matrices to a finite dimension (N), which indicates how many transverse modes propagate through the structure. This dimension is related to the maximum working frequency and goes up on increasing this frequency. We verified by means of numerical experiments hereafter proposed that in practical cases only a few modes are useful to describe the propagation in our structure. Nevertheless we verified that the inversion procedure of the truncate matrices is well behaved and stable: we shall say that an N-th–order inverse has been found if the elements of an N-th–order matrix formed by truncating the inverse matrix of an $(N + M)$-th–order solution does not change appreciably as M increased.

Finally we observe that if only the fundamental mode propagates in the waveguide ($w_1 = 0$) and in the cavity ($c_1 = 0$), the previous formulae can be simplified, and the reflection and transmission matrices become scalar quantities, given by

$$S_{11}(1,1) = \frac{1}{2}\left[\frac{1 - j\alpha\,\mathrm{tg}\,(kL)}{1 + j\alpha\,\mathrm{tg}\,(kL)} + \frac{1 + j\alpha\,\mathrm{ctg}\,(kL)}{1 - j\alpha\,\mathrm{ctg}\,(kL)}\right],$$

$$S_{12}(1,1) = \frac{1}{2}\left[\frac{1 - j\alpha\,\mathrm{tg}\,(kL)}{1 + j\alpha\,\mathrm{tg}\,(kL)} - \frac{1 + j\alpha\,\mathrm{ctg}\,(kL)}{1 - j\alpha\,\mathrm{ctg}\,(kL)}\right],$$

where $\alpha = \ln(b/a)/\ln(c/a)$.

6. – Ohmic losses

Till now we have considered the contribution to the integral in integrals (2.8) due to the coupling apertures only, since the other terms are null for a perfect conducting material. If we want to complete the study of the electromagnetic coupling between the waveguide and the cavity, ohmic losses have to be introduced in the cavity walls: the tangential component of the electric field will be no more vanishing there and one can evaluate the expansion coefficient (2.8) also on the cavity surfaces. The definition of these coefficients needs the knowledge of the electric field on the cavity surface. The Leontovič boundary condition [12,13] can be used to express the (tangential) electric field over the metallic surfaces in terms of the magnetic field, given by expressions (2.3)

$$\hat{n} \times \vec{E} = \frac{1 + j}{\sigma\delta}\hat{n} \times (\vec{H} \times \hat{n}) = \zeta\, \vec{H}_{\mathrm{t}}\,, \tag{6.1}$$

wherein σ is the electric conductivity of the metallic regions,

$$\delta = \sqrt{\frac{2}{\omega\mu\sigma}}$$

is the penetration depth, and the surface impedance ζ has been introduced. In this case we include ohmic losses in a non-perturbative way.

Regarding the coefficients A_{ps}, we note that they depend on the electric field and on the inner cavity surface S. The integral can be evaluated by dividing the surface S according to the following sub-domains:

– the lateral surface S_c of the cavity ($r = c$ and $0 \leq z \leq 2L$);

– the surrounding surface S_a of the wire ($r = a$ and $0 \leq z \leq 2L$);

– the lateral surfaces of the cavity B_1 ($z = 0$ and $b \leq r \leq c$) and B_2 ($z = 2L$ and $b \leq r \leq c$).

Following the geometrical scheme listed above, the integration (2.8) can be considered as the superposition of four contributions where the first one is related to the coupling through the apertures and has been discussed in the previous section. The other ones will be discussed and evaluated below, using Leontovič condition (6.1) for the different cases.

– All along the lateral surface S_c of the cavity [$\hat{n} = \hat{r}$] we get

$$\iint_{S_c} \hat{r} \times \vec{E}\,(P) \cdot \vec{H}^*_{ps}\,(P) \mathrm{d}S = \zeta 2\pi c \sum_{m,q} A_{mq} \int_0^{2L} \vec{H}_{mq}\,(c,z) \cdot \vec{H}^*_{ps}\,(c,z) \mathrm{d}z\,.$$

Performing the trivial integration on z [14], we finally have

$$\iint_{S_c} \hat{r} \times \vec{E}\,(P) \cdot \vec{H}^*_{ps}\,(P) \mathrm{d}S = \zeta 2\pi c\, \vec{h}^c_p\,(c) \cdot \sum_m A_{ms}\, \vec{h}^c_m\,(c)\,. \tag{6.2}$$

– Repeating the same considerations along the surrounding surface S_a of the wire [$\hat{n} = -\hat{r}$], we obtain

$$\iint_{S_a} \hat{r} \times \vec{E}\,(P) \cdot \vec{H}_{ps}\,(P) \mathrm{d}S = \zeta 2\pi a\, \vec{h}^c_p\,(a) \cdot \sum_m A_{ms}\, \vec{h}^c_m\,(a)\,. \tag{6.3}$$

Summing relations (6.2) and (6.3) we get

$$\iint_{S_a+S_c} \hat{n} \times \vec{E}\,(P) \cdot \vec{H}^*_{ps}\,(P) \mathrm{d}S = \zeta \sum_m L_{pm} I_m(s)\,, \tag{6.4}$$

where the generic element of the matrix $\boldsymbol{L} = \{L_{pm}\}$ is given by

$$L_{pm} = 2\pi[c\, \vec{h}^c_p\,(c) \cdot \vec{h}^c_m\,(c) + a\, \vec{h}^c_p\,(a) \cdot \vec{h}^c_m\,(a)]\,. \tag{6.5}$$

– The contribution of the two lateral surfaces of the cavity B_1 (where $\hat{n} = -\hat{z}$) and B_2 (where $\hat{n} = \hat{z}$) can be computed using the modal expansion of the fields and the Leontovič condition (6.1) again, namely

$$\iint_{B_1+B_2} \hat{n} \times \vec{E}\,(P) \cdot \vec{H}^*_{ps}\,(P) \mathrm{d}S = \zeta \sqrt{\varepsilon_s} \sum_{m,q} A_m(q) \frac{\sqrt{\varepsilon_q}}{2L} [1 + (-1)^{s+q}] B_{pm}\,, \tag{6.6}$$

where the symmetric matrix $\boldsymbol{B} = \{B_{nm}\}$ is defined and evaluated in Appendix B.

Summarising the previous results and representing the symmetric matrix [15]

$$\text{diag}\,[k_p^2] + j\frac{\zeta}{\zeta_0} k\boldsymbol{L} = \boldsymbol{U}\boldsymbol{D}\boldsymbol{U}^{-1} \tag{6.7}$$

by means of the eigenvalues diagonal matrix, $\boldsymbol{D} = \text{diag}\,[\lambda_p^2]$, which corresponds to the eigenvectors matrix $\boldsymbol{U}$, the elements of the scattering matrix can be written in forms similar to eqs. (5.3) and (5.4), following the same scheme outlined in the previous section; new matrices have to be defined that take into account the losses

$$\boldsymbol{E} = j\boldsymbol{Z}_{\text{w}}\boldsymbol{C}^T \left[\boldsymbol{U}\boldsymbol{Z}\,\text{tg}\,(kL\boldsymbol{Z})\boldsymbol{U}^{-1} + j\frac{\zeta}{\zeta_0}\boldsymbol{B}\right]^{-1}\boldsymbol{C}\,, \tag{6.8}$$

$$\boldsymbol{O} = j\boldsymbol{Z}_{\text{w}}\boldsymbol{C}^T \left[\boldsymbol{U}\boldsymbol{Z}\,\text{ctg}\,(kL\boldsymbol{Z})\boldsymbol{U}^{-1} - j\frac{\zeta}{\zeta_0}\boldsymbol{B}\right]^{-1}\boldsymbol{C}\,,$$

$$\boldsymbol{Z} = \text{diag}\left[\frac{\sqrt{k^2-\lambda_p^2}}{k}\right].$$

It is worth noting that these new matrices (6.8) give again the old ones (4.10) in the case $\sigma = \infty$ (perfectly conducting case) and the eigenvalues λ_p fall back in the transverse eigenvalues k_p. Ohmic losses change the cavity eigenvalues, acting as a sort of source diffused on the cavity walls. In this way, the coefficients A_{ps} contain all the information regarding the losses and the apertures.

7. – Numerical results and approximations

We started the numerical experiments with a cavity defined by the following inner and outer diameter, length and external waveguide diameter:

$$2a = 0.75\text{ mm}, \quad 2c = 25.02\text{ cm}, \quad 2L = 37.71\text{ cm}, \quad 2b = 6.87\text{ cm}\,,$$

with all the metallic regions exhibiting an electrical conductivity $\sigma = 58$ MS/m (Copper). We decided to examine the spectrum of some elements of the scattering matrix up to 4 GHz. Therefore we studied the convergence of the proposed method around 1 GHz and the maximum working frequency in order to estimate the minimum order of the scattering matrix. Figures 2 and 3 distinctly indicate that small matrices rank stabilise the scattering parameters. This implies that we are able to examine the transmission element $S_{12}(1,1)$ up to 4 GHz with high accuracy by inverting a matrix of dimension four. Similarly around a resonance frequency for $S_{12}(1,1)$, fig. 4 shows that 20 elements give the numerical evaluation with a good accuracy.

8. – Experimental results and comparison

The coaxial-wire method [6, 7, 16, 17] is a well-known technique used to characterise electromagnetic structures, which have to be inserted in particle accelerators, by measuring their transmission scattering matrix. The Device Under Test is transformed in a coaxial structure by introducing a wire on its longitudinal axis.

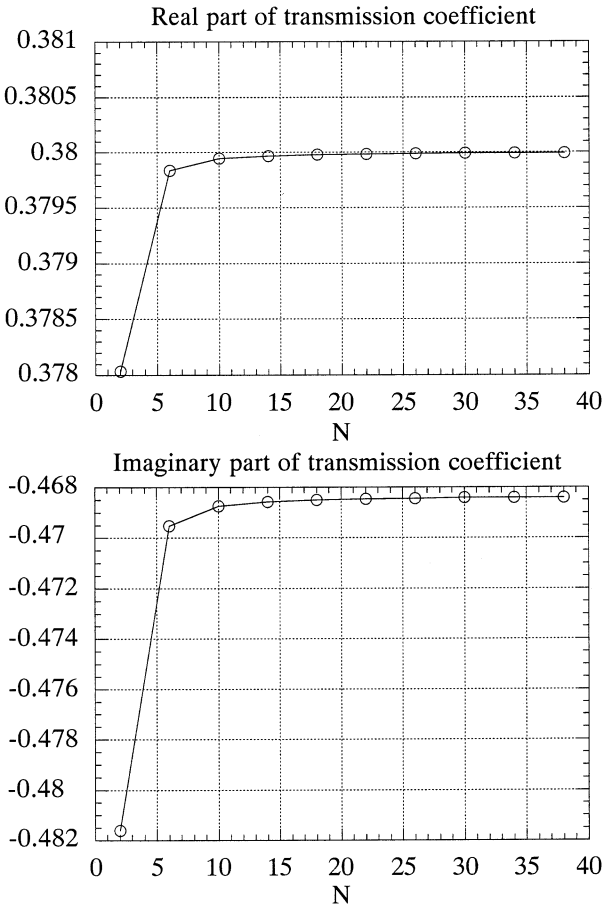

Fig. 2. – Convergence of transmission coefficient at 1 GHz.

In [5] a general relationship between the scattering matrix and the coupling impedance is given in which the S_{12} coefficient is calculated, without approximations, as referred to the DUT characteristic impedance and not to the external measurement apparatus (typically 50 Ω). Even if this method is usually used to evaluate the unknown coupling impedance of a bunch travelling the same structure, some care has to be taken in the result evaluation, because the wire presence modifies the electromagnetic field behaviour. The validity of the coaxial wire method has been investigated in some cases [8].

In order to look for an experimental validation of the MMT we perform our measurements in the frequency domain [7, 18], acquiring the transmission scattering matrix of the device (DUT) and of a reference line (REF), which has the same length as the cavity and radius equal to the small aperture shown in fig. 1. The simulation runs have been performed on a cavity with the same geometry of the measured one.

A Network Analyzer Hp 8719C (50 MHz–13.5 GHz) has been used for the measurements in the range 0–4 GHz. The instrument gives directly the scattering parameters. A computer is connected through a HP-IP bus to the instrumentation for its control and for the acquisition of the data, real and imaginary parts of the S_{ij} parameters (Labview

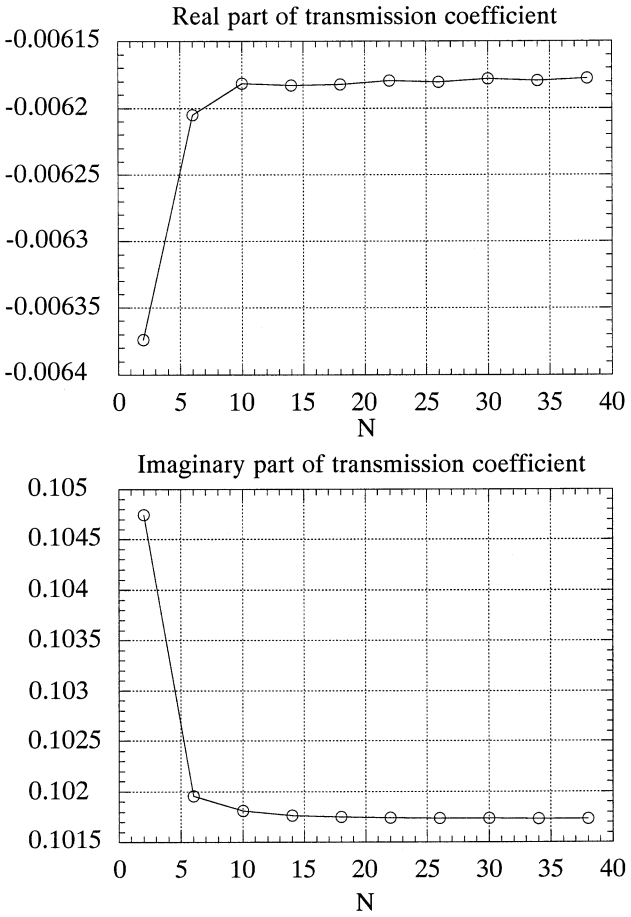

Fig. 3. – Convergence of transmission coefficient at 4 GHz.

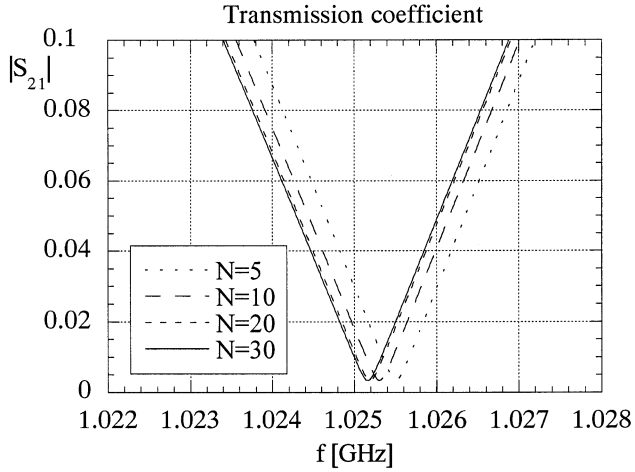

Fig. 4. – Convergence of the proposed method around the first resonance.

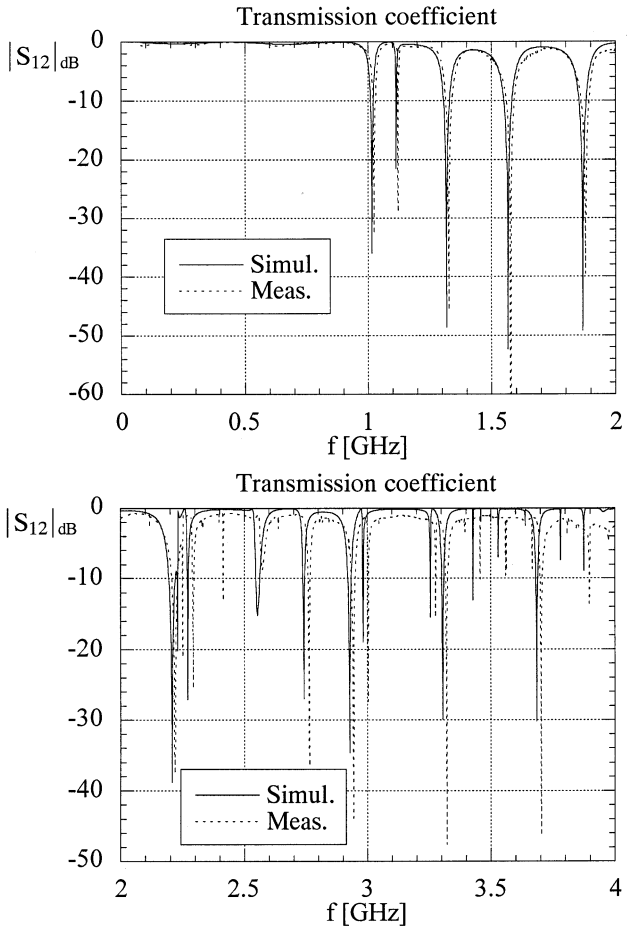

Fig. 5. – Transmission scattering coefficient: comparison between theory and measurements.

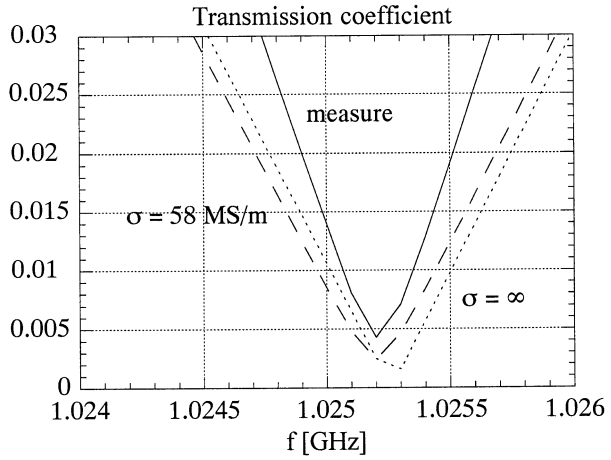

Fig. 6. – Comparison between measured and theoretical data of the first resonance.

environment). An accurate calibration has been performed for the entire band of acquisition including all the cables and the connectors. Both the REF and the DUT structures have geometrical and electrical impedance adapters in order to minimise the reflections and to improve the signal-to-noise ratio. Because some resonances could be really small and because we want well characterise the sample structure, we need a clean signal. For this reason the adapter system, mechanical and electrical, has to be carefully set up. The wire thickness (0.75 mm) was for us a good compromise between the possibility of acquiring a good signal and the requirement of not perturbing the cavity fields behaviour.

Figure 5 shows the comparison between the experimental data and the simulations performed in the same range of frequencies. The agreement is really good also for some small resonances.

In order to better understand the quality of the agreement, level and frequency values, we studied some resonances. In fig. 6 the comparison between the experimental and simulation data is reported for the first resonance, considering the effect of losses. Again the agreement is satisfactory also because we can recognise the same frequency value and the same pick level. The comparison on the resonances level gives us a way to understand the accurateness of the measure.

9. – Conclusions and perspectives

The analysis of the coupling between a feeding coaxial cable and a coaxial circular cavity has been developed by taking into account all the modes in the cable and in the cavity. An explicit formula has been obtained for the scattering matrix, which provides a simple and accurate tool for studying the coupling, and for allowing the design of such a structure without using a cumbersome numerical analysis. Finally, the comparison with the experimental results has shown both the reliability of the implemented theoretical tool and the possibility to perform very precise bench measurements of the scattering matrix. At the same time we got a good starting point for the understanding of all the existing differences between impedance measurements with the bunch and with the coaxial-wire method.

Appendix A.

Aim of this appendix is to discuss the evaluation and some properties of the coefficients

$$C_{pq} = \int_A \Phi_p^{\mathrm{c}}(r)\Phi_q^{\mathrm{w}}(r)\mathrm{d}S = 2\pi \int_a^b \Phi_p^{\mathrm{c}}(r)\Phi_q^{\mathrm{w}}(r) r \mathrm{d}r\,, \tag{A.1}$$

which take into account the coupling due the apertures among the modes of the waveguide and of the cavity. Using the remarkable integral [14]

$$\int^r x Z_p(\alpha x) B_p(\beta x)\mathrm{d}x = \frac{\beta r Z_p(\alpha r) B_{p-1}(\beta r) - \alpha r Z_{p-1}(\alpha r) B_p(\beta r)}{\alpha^2 - \beta^2}\,, \tag{A.2}$$

where $Z_p(x)$ and $B_p(x)$ are linear combination of Bessel functions, we have (p, $q \geq 2$)

$$C_{pq} = \frac{\pi x_p^2 J_0(w_q)}{(w_q^2 - x_p^2) J_0(b w_q/a)} \frac{J_0(b x_p/a) Y_0(x_p) - Y_0(b x_p/a) J_0(x_p)}{\sqrt{J_0^2(w_q)/J_0^2(b w_q/a) - 1}\sqrt{J_0^2(x_p)/J_0^2(c x_p/a) - 1}}\,, \tag{A.3}$$

where w_q and x_p are the transverse eigenvalues of the waveguide and of the cavity respectively, namely they are solution of eq. (2.7) with $\alpha = b/a$ and $\alpha = c/a$.

The elements of the first row and the first column of the matrix $\boldsymbol{C}$ are related to the fundamental mode (TEM). We get for the first row and the first column

$$C_{1q} = \sqrt{\frac{2\pi}{\ln(c/a)}} \int_a^b \Phi_q^{\mathrm{w}}(r)\mathrm{d}r = 0, \quad \text{for } q = 2, 3, 4, \dots , \tag{A.4}$$

$$C_{p1} = \sqrt{\frac{2\pi}{\ln(b/a)}} \int_a^b \Phi_p^{\mathrm{c}}(r)\mathrm{d}r = \pi \frac{J_0(x_p)Y_0(bx_p/a) - J_0(bx_p/a)Y_0(x_p)}{\sqrt{2\ln(b/a)}\sqrt{J_0^2(x_p)/J_0^2(cx_p/a) - 1}}, \quad \text{for} \quad p = 2, 3, 4, \dots \tag{A.5}$$

Finally the element C_{11} is given by

$$C_{11} = \frac{1}{\sqrt{\ln(b/a)\ln(c/a)}} \int_a^b \frac{\mathrm{d}r}{r} = \sqrt{\frac{\ln(b/a)}{\ln(c/a)}} . \tag{A.6}$$

Appendix B.

In this appendix we perform the evaluation of the coefficients

$$B_{nm} = \iint_B \Phi_n^{\mathrm{c}}(r)\Phi_m^{\mathrm{c}}(r)\mathrm{d}S = 2\pi \int_b^c \Phi_n^{\mathrm{c}}(r)\Phi_m^{\mathrm{c}}(r) r \, \mathrm{d}r . \tag{B.1}$$

From this definition it follows immediately that the matrix $\boldsymbol{B}$ is symmetric. Thus, starting with the first element B_{11}, it is

$$B_{11} = \frac{1}{\ln(c/a)} \int_b^c \frac{\mathrm{d}r}{r} = \frac{\ln(c/b)}{\ln(c/a)} . \tag{B.2}$$

We continue with the other elements of the first row (the first column) [14]

$$B_{1m} = \sqrt{\frac{2\pi}{\ln(c/a)}} \int_b^c \Phi_m^{\mathrm{c}}(r)\mathrm{d}r = \pi \frac{J_0(bx_m/a)Y_0(x_m) - J_0(x_m)Y_0(bx_m/a)}{\sqrt{2\ln(c/a)}\sqrt{J_0^2(x_m)/J_0^2(cx_m/a) - 1}} , \tag{B.3}$$

and the other off-diagonal elements, using the integral (A.2), are

$$B_{nm} = \sqrt{2\pi \ln(c/a)} b \frac{x_n^2 B_{1n}\Phi_m^{\mathrm{c}}(b) - x_m^2 B_{1m}\Phi_n^{\mathrm{c}}(b)}{x_n^2 - x_m^2} . \tag{B.4}$$

The elements of the main diagonal can be obtained from the last relation in the limit $x_n \to x_m$, namely

$$B_{nn} = \sqrt{2\pi \ln(c/a)} b \, B_{1n}\Phi_n^{\mathrm{c}}(b) .$$

REFERENCES

[1] Heifets S. A. and Kheifets S. A., *Rev. Mod. Phys.*, **63** (1991) 631.
[2] Palumbo L., Vaccaro V. G. and Zobov M., *Wake fields and impedance*, LNF-94/041(P), 5 September 1994; CERN 95-06 report of the CAS, November 1995.
[3] Vaccaro V. G., CERN ISR-RF/66-35, 1966.
[4] Chao A. W., SLAC PUB-2946, 1982.
[5] Vaccaro V. G., *Coupling measurements: an improved wire method*, INFN/TC-94/023, 1994.
[6] Walling L. S., Mc Murry D. E., Neuffer D. V. and Thiessen H. A., *Nucl. Instrum. Methods A*, **281** (1989) 433.
[7] Galluccio F., Masullo M. R., Vaccaro V. G., Schwingenheuer B., Klefenz F., Wanzenberg R. and Wendt M., *Measurement of the longitudinal coupling impedance of the Hera-B vertex detector chamber, EPAC-96, Sitges* (*Barcellona*)*, June 1996*.
[8] Gluckstern R. L. and Li R., *Particle Accelerators*, **29** (1990) 159.
[9] Collin R. E., *Foundations for Microwave Engineering* (McGraw-Hill, New York) 1992.
[10] Lee S. W. and Mittra R., *Analytical Techniques in the Theory of Guided Waves* (The Macmillan Company, New York) 1971.
[11] Bucci O. M. and Di Massa G., *Open resonators powered by a rectangular waveguide, IEE Proceedings-II*, **139**(4), August 1992.
[12] Franceschetti G., *Campi elettromagnetici* (Boringhieri, Torino) 1983.
[13] Marcuvitz N., *Waveguide handbook, IEE Electromagnetic Waves Series* (New York) 1950.
[14] Gradshteyn I. S. and Ryzhik I. M., *Table of Integrals, Series, and Products* (Academic Press, New York) 1980.
[15] Gantamacher F. M., *Applications of the Theory of Matrices* (Wiley, New York) 1959.
[16] Sands M. and Rees J. R., *A bench measurement of the energy loss of a stored beam to a cavity*, SLAC report PEP-0095, 1975.
[17] Hahn H. and Pedersen F., Brookhaven National Laboratory report BNL-50870, April 1978.
[18] Davino D., Masullo M. R., Vaccaro V. G. and Verolino L., *Mode matching technique for a lossy pill-box cavity, EPAC-98, Stockholm, June 1998*.